Research Square

Preprints are preliminary reports that have not undergone peer review.
They should not be considered conclusive, used to inform clinical practice,
or referenced by the media as validated information.

Circulating Tfh-Related Immune Profiles and Clinical Associations of Plasma CXCL13 in Esophageal Cancer

SIQI LONG
Affiliated Hospital of North Sichuan Medical College
YUNFENG LV
North Sichuan Medical College
BIN GUO
North Sichuan Medical College
GUANGCHENG LUO
Affiliated Hospital of North Sichuan Medical College
QI LIANG
North Sichuan Medical College
Maisarah Abdul Mutalib
maisarah_abdulmutalib@msu.edu.my
Management and Science University

Research Article

Keywords: esophageal cancer, circulating follicular helper T cells, CXCL13, follicular regulatory T cells

Posted Date: August 21st, 2026

DOI: https://doi.org/10.21203/rs.3.rs-10381612/v1

License: This work is licensed under a Creative Commons Attribution 4.0 International License.
Read Full License

Additional Declarations: No competing interests reported.

Abstract

Objective

To assess perioperative differences in circulating $CD4^+CXCR5^+$ T cells, CD25-based regulatory phenotypes, and plasma C-X-C motif chemokine ligand 13 (CXCL13) in esophageal cancer (ESCA), and to evaluate their clinical relevance.

Methods

Fifty patients with ESCA (29 preoperative and 21 postoperative patients), and 24 healthy controls were enrolled. Circulating $CD4^+CXCR5^+$ T cells, $CD4^+CD25^+$ Treg phenotypes, and $CD4^+CXCR5^+CD25^+$ Tfr phenotypes were quantified by flow cytometry, and plasma CXCL13 was measured by enzyme-linked immunosorbent assay. Clinicopathological and survival associations were evaluated in the preoperative cohort using correlation analysis, Kaplan–Meier estimation, and exploratory Cox regression.

Results

Compared with healthy controls, preoperative patients had higher frequencies of circulating $CD4^+CXCR5^+$ T cells and the $CD4^+CD25^+$ Treg phenotype, whereas plasma CXCL13 levels were higher in both patients cohort. Postoperative patients had lower frequencies of circulating $CD4^+CXCR5^+$ T cells, the $CD4^+CXCR5^+CD25^+$ Tfr phenotype, and the $CD4^+CD25^+$ Treg phenotype than preoperative patients. In preoperative patients, $CD4^+CXCR5^+$ T-cell frequency correlated positively with Treg and Tfr phenotypes ($r = 0.50$ and 0.56; both $P < 0.01$). Plasma CXCL13 was higher in T3–T4 than T1–T2 disease ($P = 0.022$). High preoperative CXCL13 was associated with shorter overall survival (log-rank $P = 0.018$) and remained significant in an exploratory Cox model (adjusted HR = 5.50, 95% CI 1.06–28.56; $P = 0.043$).

Conclusions

Circulating Tfh-related and regulatory phenotypes differed across study groups, whereas plasma CXCL13 was elevated in both patient groups. Higher preoperative CXCL13 was associated with deeper tumor invasion and shorter overall survival, supporting further evaluation as an accessible biomarker.

1. Introduction

Esophageal cancer (ESCA) remains a major cause of cancer-related mortality worldwide [1]. Early clinical manifestations are often non-specific or subtle, and many patients are diagnosed only after progression to advanced stages. Currently, diagnosis and staging largely depend on endoscopic evaluation with histopathological confirmation, which is invasive and unsuitable for repeated monitoring or population-level screening, and limited in its ability to detect early lesions with high sensitivity and

specificity [2]. Collectively, these challenges highlight the need for non-invasive, readily repeatable circulating biomarkers to enable earlier detection, refine risk stratification, and enable longitudinal monitoring.

The tumor immune microenvironment (TIME) plays a pivotal role in cancer progression and therapeutic response. Tertiary lymphoid structures (TLS) are widely recognized as functional "ectopic immune centers" within the TIME. Mature TLS, which contain germinal centers, enhance local antitumor immunity by organizing antigen presentation, facilitating interactions between follicular helper T (Tfh) cells and B cells, and supporting local humoral immune responses. Their presence has been associated with improved immunotherapy response and survival [3], [4]. TLS initiation and maintenance are regulated by coordinated chemokine programs, among which the CXCR5-CXCL13 axis is a central pathway that recruits Tfh cells and supports germinal-center–like B-cell responses. Tfh cells secrete CXCL13, which recruits and organizes B cells to form functional germinal centers. In addition, Tfh cells produce cytokines such as interleukin-21 (IL-21), promoting affinity maturation and plasma cell differentiation, thereby strengthening humoral immunity [5].

However, the role of the Tfh-CXCL13 axis is context-dependent and not uniformly beneficial. In lung adenocarcinoma, this axis enhances CD8 + T cell cytotoxicity and memory formation through IL-21 signaling, exerting anti-tumor effects [6], [7]. In contrast, in breast cancer, CXCL13 has been linked to exhaustion-associated immune environments, where tumors harboring exhausted-like T cells show increased CXCL13 expression in T cells and altered spatial organization with immature rather than mature TLS-like structures [8]. Follicular regulatory T (Tfr) cells represent a specialized subset of regulatory T (Treg) cells. They co-express phenotypic markers of both Treg and Tfh cells and regulate germinal center responses by suppressing Tfh and B cell activity [9]. Although the prognostic value of tumour-infiltrating lymphocytes and TLS has been extensively characterized, the clinical significance of circulating Tfh and Tfr cells, as well as plasma CXCL13 levels in esophageal cancer, particularly ESCC, remains poorly understood.

In the present study, we investigated the expression profiles and clinical relevance of circulating Tfh, Tfr cells and plasma CXCL13 in patients with esophageal cancer. We compared the level of these markers between preoperative and postoperative patients and evaluated their associations with clinicopathological features, including tumor invasion depth and survival. Additionally, we examined the relationship between circulating Tfh cells and immunoregulatory (Tfr and Treg) subsets to determine whether these circulating immune features have potential prognostic relevance and reflect systemic immune regulation in ESCA

2. Materials and methods

2.1 Study population

This retrospective study included a total of 50 patients with esophageal cancer (ESCA) at the Affiliated Hospital of North Sichuan Medical College, including 29 preoperative and 21 postoperative patients. Patients were identified between February and July 2019, and healthy controls were identified from individuals undergoing routine health examinations during the same period. The preoperative and postoperative groups consisted of different patients and were therefore analyzed as independent cohorts. For all study groups, residual EDTA-anticoagulated peripheral blood remaining after completion of clinically indicated routine blood count testing was used for the study assays. No additional blood was drawn solely for research purposes. Residual preoperative specimens originated from routine blood samples obtained before surgical resection, whereas residual postoperative specimens originated from routine blood samples obtained on postoperative days 3–5. Residual specimens from healthy controls originated from routine complete blood count testing performed as part of their health examinations.

The patient cohort comprised 30 males and 20 females, aged 50–81 years. Histopathological subtypes included esophageal squamous cell carcinoma (n = 45) and esophageal adenocarcinoma (n = 5). Eligibility criteria were as follows: (a) histopathologically confirmed ESCA; (b) no prior radiotherapy, chemotherapy, or targeted therapy; and (c) absence of autoimmune diseases or severe infections. In addition, 24 healthy individuals undergoing routine health examinations during the same period were recruited as controls. There were no significant differences in age or sex distribution between the control group and the ESCA group ($P > 0.05$). Clinical data were collected, including demographic characteristics (age and sex), TNM stage, and tumor differentiation grade. Patients were followed up through review of outpatient and inpatient medical records and telephone interviews. The study was reviewed and approved by the Medical Ethics Committee of Affiliated Hospital of North Sichuan Medical College (approval no. 2026ER60-1). Because this retrospective study used residual clinical specimens remaining after routine laboratory testing and involved no additional blood collection solely for research purposes, the requirement for informed consent to participate was waived by the ethics committee.

2.2 Flow cytometry

EDTA-anticoagulated whole blood (100 μL) was aliquoted into BD flow cytometry tubes and stained with PerCP-Cy5.5–conjugated anti-human CD4 (clone L200, Cat. no. 552838, BD Biosciences), APC-conjugated anti-human CXCR5 (CD185) (clone J252D4, Cat. no. 356908, BioLegend), and PE-conjugated anti-human CD25 (clone 2A3, Cat. no. 341009, BD Biosciences). Samples were gently vortexed and incubated for 30 min at 4°C in the dark. Red blood cells were lysed with 1 mL of 1× erythrocyte lysis buffer (Cat. no. Z6910001S, Beijing Tongsheng Times Bio-Technology Co., Ltd.) for 10 min. After lysis, 1 mL phosphate-buffered saline (PBS) was added, and samples were centrifuged at 300 × g for 5 min. The supernatant was discarded, and cells were washed once with PBS and centrifuged again under the same conditions. Cells were resuspended in 400 μL PBS and acquired on a BD FACSCanto II flow cytometer (BD Biosciences). Data were analyzed using FACSDiva software.

Phenotypic definitions. Lymphocytes were first gated based on forward and side scatter properties. Within $CD4^+$ T cells, circulating Tfh cells were defined as $CD4^+CXCR5^+$ cells. The CD25-based Treg phenotype was defined as $CD4^+CD25^+$ cells, and the CD25-based Tfr phenotype was defined as

$CD4^+CXCR5^+CD25^+$ cells. The frequencies of $CD4^+CXCR5^+$ cells and $CD4^+CD25^+$ cells were calculated as percentages of gated lymphocytes, whereas the frequency of $CD4^+CXCR5^+CD25^+$ cells was calculated as a percentage of gated $CD4^+$ lymphocytes. Because intracellular FOXP3 staining and CD127-based refinement were not performed, these CD25-based definitions were used as phenotypic surrogates for regulatory subsets.

2.3 CXCL13 measurement

Plasma CXCL13 concentrations were quantified using a commercially available sandwich ELISA kit for human CXCL13 (Cat. no. DCX130, R&D Systems, Minneapolis, MN, USA), following the manufacturer's instructions. Plasma samples were thawed at room temperature, gently mixed, and clarified by centrifugation at 1000 xg for 10 min to remove particulates before analysis. Standards of known concentrations and plasma samples were added to microplate wells preloaded with assay diluent and incubated, followed by washing steps to remove unbound material. A human CXCL13 conjugate was then added and incubated. After additional washing steps, a substrate solution was added to initiate color development. The optical density (OD) was measured at 450 nm using a microplate reader (Model PHOmo, Autobio Diagnostics, Zhengzhou, China). A standard curve was generated by fitting OD values to the corresponding standard concentrations, and plasma CXCL13 concentrations in the samples were calculated from the resulting calibration curve.

2.4 Expression of CXCR5 and CXCL13 in ESCA from TCGA database

The mRNA expression of CXCR5 and CXCL13 in esophageal carcinoma (ESCA) was analysed using the Gene Expression Profiling Interactive Analysis (GEPIA) web server[10](http://gepia.cancer-pku.cn; accessed December 17, 2025). Tumor–normal expression boxplots were generated for the TCGA-ESCA cohort using the option **"Match TCGA normal and GTEx data"** for normal tissue comparison. Expression values were displayed on the log scale (log2[TPM + 1]), with thresholds set at |log2FC| = 1 and P = 0.01 (jitter size = 0.4). The association between CXCR5 and CXCL13 expression was assessed using the "Correlation Analysis" module of GEPIA in ESCA tumor samples. Pearson correlation was applied. Correlation coefficients were calculated by GEPIA using non-log–transformed expression values, while the scatterplot was displayed on the log2(TPM) scale as implemented by the platform. This analysis was performed to provide tissue-level transcriptomic context for CXCL13 and CXCR5 expression in ESCA.

2.5 Statistical analysis

Statistical analyses were performed using IBM SPSS Statistics software package, version 23.0 (IBM Corporation, Armonk, NY, USA), and graphical visualization was generated using GraphPad Prism, version 9.0 (GraphPad Software Inc., San Diego, CA, USA). The normality of data distribution was assessed using the Shapiro–Wilk test. Non-normally distributed quantitative data were expressed as median (interquartile range [IQR]). Comparisons among the preoperative, postoperative, and healthy control groups were performed using the Kruskal–Wallis H test, followed by Dunn's post hoc test with Bonferroni adjustment for pairwise comparisons. Comparisons between two independent groups in the

clinicopathological analyses were performed using the exact two-sided Mann–Whitney U test. Pearson or Spearman correlation analysis was performed, as appropriate, according to data distribution. Overall survival was estimated using the Kaplan–Meier method and compared using the log-rank test, with administrative censoring at 60 months. Hazard ratios (HRs) with 95% confidence intervals (CIs) were estimated using Cox proportional hazards regression. Given the limited number of events, the adjusted Cox model was restricted to CXCL13 group and T stage. All statistical tests were two-sided, and $P < 0.05$ was considered statistically significant.

3. Results

3.1 Differences in circulating CD4⁺CXCR5⁺ T cells, CD25-based regulatory phenotypes, and plasma CXCL13 across study groups

To characterize circulating CXCR5/CXCL13-associated immune features in ESCA, we quantified circulating CD4⁺CXCR5⁺ T cells, operationally defined as circulating Tfh cells, together with CD25-based regulatory phenotypes, including the CD4⁺CD25⁺ Treg phenotype and the CD4⁺CXCR5⁺CD25⁺ Tfr phenotype. As shown in Table 1 and Fig. 1, preoperative patients exhibited significantly higher frequencies of circulating CD4⁺CXCR5⁺ T cells and the CD4⁺CD25⁺ Treg phenotype than healthy controls. Plasma CXCL13 levels were also significantly higher in both preoperative and postoperative patients than in healthy controls (all adjusted $P < 0.05$). In contrast, the CD4⁺CXCR5⁺CD25⁺ Tfr phenotype did not differ significantly between either patient group and healthy controls.

We next compared the independent preoperative and postoperative cohorts. Postoperative patients sampled on postoperative days 3–5 had significantly lower frequencies of circulating CD4⁺CXCR5⁺ T cells, the CD4⁺CXCR5⁺CD25⁺ Tfr phenotype, and the CD4⁺CD25⁺ Treg phenotype than preoperative patients (all adjusted $P < 0.05$). Plasma CXCL13 levels did not differ significantly between the preoperative and postoperative groups (adjusted $P > 0.05$).

Table 1
Comparison of circulating CD4⁺CXCR5⁺ T cells, CD25-based regulatory phenotypes, and plasma CXCL13 levels among preoperative patients, postoperative patients, and healthy controls

Groups	n	Tfh (%)	Tfr phenotype (%)	Treg phenotype (%)	CXCL13 (pg/mL)
Preoperative	29	9.2 (6.1–12.3)[ab]	0.6 (0.4–0.8)[b]	2.8 (2.0-3.7)[ab]	161.4 (125.8-216.8)[a]
Postoperative	21	6.0 (4.9–7.8)	0.4 (0.2–0.5)	2.0 (1.4–2.6)	187.6 (140.1-292.4)[a]
HC	24	6.2 (5.5–7.6)	0.4 (0.3–0.7)	1.9 (1.2–2.2)	102.8 (87.4-124.1)

Notes: Data are presented as median (interquartile range [IQR]). Overall differences among the three independent groups were assessed using the Kruskal–Wallis H test, followed by Dunn's post hoc test with Bonferroni adjustment for pairwise comparisons. $CD4^+CXCR5^+$ and $CD4^+CD25^+$ frequencies are expressed as percentages of gated lymphocytes, whereas $CD4^+CXCR5^+CD25^+$ frequencies are expressed as percentages of gated $CD4^+$ lymphocytes. HC, healthy controls; ESCA, esophageal cancer; Tfh, $CD4^+CXCR5^+$ T cells operationally defined as circulating Tfh cells; Tfr phenotype, $CD4^+CXCR5^+CD25^+$ cells; Treg phenotype, $CD4^+CD25^+$ cells; CXCL13, C-X-C motif chemokine ligand 13. CD25-based regulatory phenotypes were used as phenotypic surrogates for regulatory subsets because FOXP3 staining and CD127-based refinement were not performed.

 Adjusted $P < 0.05$ versus the HC group.

 Adjusted $P < 0.05$ versus the postoperative group.

3.2 Coordinated variation between circulating $CD4^+CXCR5^+$ T cells and CD25-based regulatory phenotypes

Given the biological link between CXCR5 + Tfh cells and their ligand CXCL13, we initially investigated their correlation in the peripheral circulation of preoperative patients (Fig. 2A). Spearman correlation analysis revealed that plasma CXCL13 concentrations were not significantly correlated with the frequencies of circulating T-cell subsets ($P > 0.05$; Fig. 2A).

However, a distinct pattern of association emerged among cellular subsets. Circulating CD4 + CXCR5+ Tfh cell frequencies were positively correlated with the CD4 + CD25+ Treg phenotype ($r = 0.50$, $P < 0.01$; Fig. 2B) and with the CD4 + CXCR5+CD25 + Tfr phenotype ($r = 0.56$, $P < 0.01$; Fig. 2C). These findings indicate coordinated variation between circulating CD4 + CXCR5+ Tfh cells and CD25-based regulatory phenotypes in ESCA.

(A) Heatmap showing the Spearman correlation matrix among circulating $CD4^+CXCR5^+$ T cells, the $CD4^+CD25^+$ Treg phenotype, the $CD4^+CXCR5^+CD25^+$ Tfr phenotype, and plasma CXCL13 levels in preoperative ESCA patients. The numbers within the cells represent Spearman's correlation coefficients (r). (B) Scatter plot showing a positive correlation between circulating $CD4^+CXCR5^+$ T-cell frequencies and the $CD4^+CD25^+$ Treg phenotype ($r = 0.50$, $P < 0.01$). (C) Scatter plot showing a positive correlation between circulating $CD4^+CXCR5^+$ T-cell frequencies and the $CD4^+CXCR5^+CD25^+$ Tfr phenotype ($r = 0.56$, $P < 0.01$). Tfh, $CD4^+CXCR5^+$ T cells operationally defined as circulating Tfh cells; Treg phenotype, $CD4^+CD25^+$ cells; Tfr phenotype, $CD4^+CXCR5^+CD25^+$ cells; CXCL13, C-X-C motif chemokine ligand 13; ESCA, esophageal cancer. $P < 0.05$ was considered statistically significant.

3.3 High plasma CXCL13 levels are associated with tumor invasion and shorter overall survival

To investigate the clinical relevance of these immune markers, we performed a subgroup analysis in 26 preoperative ESCA patients with complete clinicopathological data. Three of the 29 preoperative patients

were excluded from analyses requiring T-stage information because their T stage was unavailable. As shown in Table 2, the frequencies of circulating $CD4^+CXCR5^+$ T cells, the CD25-based Treg phenotype, and the CD25-based Tfr phenotype, as well as plasma CXCL13 levels, were not significantly associated with sex or age. No significant associations were observed between these immune markers and tumor differentiation, although the CD25-based Tfr phenotype showed a borderline trend toward higher frequencies in poor–moderately differentiated tumors compared with well-differentiated tumors (exact P = 0.0503).

Notably, plasma CXCL13 levels were significantly associated with tumor invasion depth. Patients with advanced T stage disease (T3–T4) exhibited higher plasma CXCL13 levels than those with early T stage disease (T1–T2) (174.0 [156.4–238.1] vs. 126.8 [102.7–178.4] pg/mL, P = 0.022; Table 2 and Fig. 3A). In contrast, circulating $CD4^+CXCR5^+$ T-cell frequencies and CD25-based regulatory phenotypes were not significantly associated with T stage.

We further evaluated the prognostic relevance of plasma CXCL13 in the preoperative cohort with available follow-up data (n = 29). Overall survival was analyzed with administrative censoring at 60 months. Patients were stratified according to the median preoperative plasma CXCL13 concentration into a CXCL13-high group (≥ 161.44 pg/mL, n = 15) and a CXCL13-low group (< 161.44 pg/mL, n = 14). Kaplan–Meier analysis showed that patients in the CXCL13-high group had significantly shorter OS than those in the CXCL13-low group (log-rank P = 0.018; Fig. 3B), with 60-month OS rates of 20.0% and 71.4%, respectively. Univariable Cox regression further showed that high plasma CXCL13 was associated with a higher hazard of death within 60 months (HR = 3.59, 95% CI: 1.15–11.27, P = 0.028). Analyses involving T stage were based on complete cases and included 26 patients with 13 deaths. Advanced T stage showed a borderline association with shorter OS in univariable Cox analysis (HR = 3.12, 95% CI: 0.96–10.16, P = 0.059). Given the limited number of events, an exploratory bivariable Cox model including only CXCL13 group and T stage was constructed to reduce overfitting. In this model, high plasma CXCL13 remained associated with shorter OS after adjustment for T stage (adjusted HR = 5.50, 95% CI: 1.06–28.56, P = 0.043), whereas T stage was not significantly associated with OS after adjustment for CXCL13 group (adjusted HR = 1.53, 95% CI: 0.42–5.53, P = 0.516). These findings suggest that elevated plasma CXCL13 may be associated with adverse survival outcomes in preoperative ESCA patients, although the wide confidence intervals indicate limited precision due to the small sample size.

(A) Plasma CXCL13 levels were compared between patients with early tumor invasion stage (T1–T2, n = 13) and advanced tumor invasion stage (T3–T4, n = 13). (B) Kaplan–Meier analysis of overall survival (OS) in preoperative ESCA patients with available follow-up data (n = 29), stratified according to the median plasma CXCL13 concentration. Patients were categorized into the CXCL13-high group (≥ 161.44 pg/mL, n = 15) and CXCL13-low group (< 161.44 pg/mL, n = 14). Overall survival was administratively censored at 60 months. Survival curves were compared using the log-rank test. The hazard ratio (HR) and 95% confidence interval (CI) were estimated using univariable Cox proportional hazards regression. CXCL13, C-X-C motif chemokine ligand 13; ESCA, esophageal cancer.

Table 2
Associations between circulating immune markers and clinicopathological characteristics in preoperative ESCA patients.

Characteristic	Subgroup	n	Tfh (%)	Treg phenotype (%)	Tfr phenotype (%)	CXCL13 (pg/mL)
Sex	Male	15	8.6 (4.1–12.8)	2.4 (1.9–3.4)	0.5 (0.4–0.7)	161.4 (118.4–212.0)
	Female	11	9.8 (7.2–11.2)	3.0 (2.3–4.1)	0.7 (0.5–0.9)	162.1 (126.8–235.4)
	P value		0.83	0.36	0.09	0.57
Age, years	≥ 70	10	8.2 (4.1–12.4)	2.5 (2.1–3.8)	0.6 (0.4–0.9)	183.0 (147.4–252.1)
	< 70	16	9.4 (7.2–11.1)	2.8 (1.9–3.8)	0.6 (0.4–0.8)	149.7 (119.6–201.4)
	P value		0.73	0.91	0.85	0.08
T stage	T1–T2	13	8.2 (5.1–10.7)	2.6 (1.9–3.3)	0.5 (0.3–0.7)	126.8 (102.7–178.4)
	T3–T4	13	10.3 (5.2–12.9)	2.9 (2.2–4.2)	0.7 (0.5–0.9)	174.0 (156.4–238.1)
	P value		0.10	0.41	0.14	**0.02**
Differentiation	Poor–moderate	11	9.7 (7.2–12.3)	3.1 (2.3–4.1)	0.7 (0.6–0.9)	169.6 (132.6–240.8)
	Well	15	8.6 (4.1–12.2)	2.3 (1.8–3.3)	0.5 (0.3–0.7)	152.3 (118.4–192.0)
	P value		0.62	0.13	0.05	0.24

Notes: Data are presented as median (interquartile range). Only preoperative patients with complete clinicopathological data were included (n = 26). Comparisons between two groups were performed using the exact two-sided Mann–Whitney U test. Tfh, $CD4^+CXCR5^+$ T cells operationally defined as circulating Tfh cells; Treg phenotype, $CD4^+CD25^+$ cells; Tfr phenotype, $CD4^+CXCR5^+CD25^+$ cells; CXCL13, C-X-C motif chemokine ligand 13; ESCA, esophageal cancer. Bold values indicate statistical significance ($P < 0.05$). The exact P value for the comparison of Tfr phenotype by differentiation was 0.0503 and was not considered statistically significant.

3.4 Public transcriptomic analysis of CXCL13 and CXCR5 in ESCA

To provide tissue-level transcriptomic context for the circulating CXCL13 findings, we analyzed transcriptomic data from the TCGA and GTEx databases using the GEPIA platform. CXCL13 and CXCR5 mRNA expression levels were significantly higher in ESCA tumor tissues (n = 182) than in normal tissues (n = 286) (both $P < 0.05$, Fig. 4A,B), consistent with the observed elevation of circulating CXCL13 levels. In addition, CXCR5 expression was positively correlated with CXCL13 expression across ESCA tumor samples ($r = 0.36$, $P < 0.01$; Fig. 4C), suggesting coordinated expression of the CXCR5-CXCL13 axis at the transcriptomic level.

(A, B) Box plots showing CXCR5 (A) and CXCL13 (B) mRNA expression in TCGA-ESCA tumor tissues (n = 182) and normal esophageal tissues from TCGA and GTEx (n = 286), as analyzed using GEPIA. Expression values are presented as $\log_2(TPM + 1)$. $P < 0.05$. (C) Pearson correlation analysis between CXCL13 and CXCR5 expression in TCGA-ESCA tumor tissues. CXCL13 expression was positively correlated with CXCR5 expression (Pearson's $R = 0.36$, $P = 8.3 \times 10^{-7}$). CXCL13, C-X-C motif chemokine ligand 13; CXCR5, C-X-C chemokine receptor type 5; ESCA, esophageal cancer; TPM, transcripts per million.

4. Discussion

Esophageal cancer is characterized by inflammation-associated tumorigenesis and an immunoregulatory tumor microenvironment that can limit effective antitumor immunity and therapeutic response [11]. In this study, we adopted a clinically feasible peripheral blood–based strategy to evaluate CXCR5/CXCL13-associated immune features in ESCA. We quantified circulating $CD4^+CXCR5^+$ T cells (operationally defined as Tfh cells), CD25-based regulatory phenotypes (the $CD4^+CD25^+$ Treg phenotype and $CD4^+CXCR5^+CD25^+$ Tfr phenotype), and plasma CXCL13. Their perioperative patterns and clinicopathological correlates were subsequently assessed. Compared with healthy controls, preoperative patients exhibited higher circulating $CD4^+CXCR5^+$ T-cell and $CD4^+CD25^+$ Treg phenotype frequencies, whereas plasma CXCL13 levels were higher in both preoperative and postoperative patients. Early postoperative patients had lower frequencies of circulating $CD4^+CXCR5^+$ T cells and CD25-based regulatory phenotypes than preoperative patients. Circulating $CD4^+CXCR5^+$ frequencies were positively associated with CD25-based regulatory phenotypes, and higher plasma CXCL13 levels were associated with deeper tumor invasion and shorter overall survival. After adjustment for T stage in an exploratory Cox model, high plasma CXCL13 remained associated with poorer survival, although the confidence interval was wide. Collectively, these findings indicate systemic alterations in follicular-associated immune features in ESCA and suggest that plasma CXCL13 may serve as a clinically relevant correlate of adverse disease features, warranting further validation.

Tfh cells and CXCL13 are commonly discussed in the context of cancer through their relationship to tertiary lymphoid structures (TLS), which organize B-cell responses and are frequently associated with improved prognosis and enhanced responses to immune checkpoint blockade [12], [13]. In ESCA, particularly ESCC, multiple studies have reported that TLS presence, spatial distribution, and maturity correlate with an inflamed tumor microenvironment and favorable clinical outcomes, and may predict

responsiveness to immunotherapy [3], [4], [14], [15]. Within this tissue-based framework, our study instead adopted a peripheral blood-based strategy and operationally defined circulating Tfh cells as $CD4^+CXCR5^+$T cells. This definition captures the broader $CD4^+CXCR5^+$ compartment rather than activated or germinal center-like Tfh subsets, which would require additional markers such as PD-1, ICOS, and CD45RA [16], [17]. This pragmatic strategy prioritizes feasibility and reproducibility in perioperative clinical sampling and enables evaluation of follicular-associated immune signals when repeated tissue acquisition or spatial analysis is not feasible. Based on this definition, Circulating $CD4^+CXCR5^+$ T-cell frequencies were lower in the early postoperative cohort than in the preoperative cohort; however, this cross-sectional difference cannot be attributed specifically to tumor resection and requires confirmation in paired longitudinal samples.

A notable observation was the coordinated variation between circulating $CD4^+CXCR5^+$ frequencies and CD25-based regulatory phenotypes. This pattern may reflect parallel induction of helper and regulatory immune programs under persistent antigenic stimulation, whereby follicular-helper-associated and regulatory compartments expand concurrently to maintain immune homeostasis [18], [19], [20]. Mechanistically, follicular regulatory T (Tfr) cells represent a specialized subset that localizes to germinal center–like niches and restrains Tfh-driven humoral responses, providing a conceptual basis for the parallel variation observed [21]. CD25 (IL-2Rα) plays a central role in high-affinity IL-2 signaling, that supports regulatory T-cell development, maintenance, and functional activity, and $CD25^{high}$ effector Treg states have been linked to suppressive programs in human tumors [22], [23]. Accordingly, our findings support a conservative interpretation in which higher circulating $CD4^+CXCR5^+$ T-cell frequencies in preoperative ESCA patients occur alongside higher CD25-based regulatory phenotype frequencies, potentially reflecting coordinated systemic immunoregulatory remodeling. Importantly, because FOXP3 staining, CD127-based refinement, and functional suppression assays were not performed, these populations should be interpreted as phenotypic regulatory compartments rather than definitive functional Treg or Tfr cells.

A further observation was the divergence between cellular and soluble immune markers in the perioperative setting. Circulating lymphoid subset frequencies differed between preoperative and postoperative cohorts, whereas plasma CXCL13 remained elevated and did not significantly differ between the two groups. Several aspects of chemokine biology may provide plausible explanations for this dissociation. CXCL13 can be retained and spatially organized through interactions with glycosaminoglycans within the extracellular matrix, influencing its distribution and persistence relative to cellular turnover. In addition, CXCL13 may be derived from non-lymphoid sources [24], including stromal compartments such as cancer-associated fibroblasts (CAFs), and may also reflect perioperative inflammatory responses. Supporting this, recent evidence indicates that fibroblast-derived signals can induce CXCL13 production in activated T cells via TGF-β–dependent pathways[25], supporting a stromal–immune circuit capable of sustaining CXCL13 levels beyond immediate changes in circulating immune cell frequencies. Clinically, the association between elevated plasma CXCL13 and deeper tumor invasion and poorer overall survival supports its potential role as a candidate liquid-phase biomarker for

risk stratification. Notably, high plasma CXCL13 remained associated with shorter OS after adjustment for T stage in an exploratory Cox model, suggesting that its prognostic relevance was not solely explained by tumor invasion depth. Nevertheless, these findings should be interpreted cautiously and require validation in larger cohorts.

Transcriptomic analyses from public datasets provided complementary evidence supporting engagement of the CXCL13/CXCR5 axis at the tissue level. Using TCGA and GTEx data via GEPIA, both CXCL13 and CXCR5 mRNA expression levels were higher in tumor tissues compared with normal tissues, and their expression was positively correlated across ESCA samples. These findings are consistent with tissue-level co-expression of the CXCL13/CXCR5 axis within the tumor microenvironment. Notably, this tissue-level association was not mirrored in peripheral blood, where plasma CXCL13 showed only weak, non-significant correlations with circulating $CD4^+CXCR5^+$ frequencies (Spearman $r = 0.12$) and with CD25-based regulatory phenotypes ($r = 0.10$ for the Tfr phenotype and $r = 0.02$ for the Treg phenotype; $P > 0.05$). This discrepancy indicates that tumor-level transcriptomic interactions and systemic circulating biomarkers reflect distinct biological layers. While tissue CXCL13/CXCR5 co-expression may represent localized immune–stromal interactions, plasma CXCL13 likely reflects a composite systemic signal influenced by multiple cellular sources, release dynamics, and clearance mechanisms. Accordingly, plasma CXCL13 should be interpreted as a clinically accessible correlate rather than a direct surrogate of circulating $CD4^+CXCR5^+$ T cell dynamics. Because the TCGA/GTEx analyses were based on bulk tissue transcriptomic data, these findings should be regarded as supportive evidence of tissue-level CXCL13/CXCR5 co-expression rather than direct validation of a Tfh-specific mechanism.

Several limitations should be acknowledged. First, the sample size was modest, which limited statistical precision and restricted the scope of adjusted survival modeling. Although high plasma CXCL13 remained associated with shorter OS after adjustment for T stage, the confidence interval was wide, and the adjusted Cox model was intentionally limited to CXCL13 group and T stage to reduce overfitting. Therefore, the prognostic relevance of plasma CXCL13 should be interpreted as exploratory rather than definitive. Second, the perioperative comparisons were cross-sectional rather than paired, limiting inference about true longitudinal postoperative immune changes. Moreover, sampling on postoperative days 3–5 may have captured acute surgical stress and postoperative inflammatory responses in addition to tumor resection-related effects. Third, the regulatory phenotypes were defined using CD25 without FOXP3 staining, CD127-based refinement, or functional validation, and thus should not be interpreted as definitive functional Treg or Tfr populations. Fourth, the study included treatment-naïve patients and did not include patients receiving immune checkpoint inhibitors; consequently, the relevance of circulating CXCL13 to immunotherapy response could not be assessed. Fifth, the cohort included both squamous cell carcinoma and adenocarcinoma, with squamous cell carcinoma predominating, and the small number of adenocarcinoma cases precluded reliable histology-specific analyses. Sixth, tumor-infiltrating lymphocytes, tissue CXCL13/CXCR5 expression, TLS status, and spatial immune organization were not evaluated. Future studies should integrate paired perioperative blood sampling, refined immunophenotyping, standardized postoperative sampling windows, histology-

stratified validation, tissue-level TLS assessment, and larger prospective cohorts with more comprehensive prognostic modeling. Given the established relevance of TLS in ESCC, incorporating spatial pathology endpoints such as TLS presence and maturation alongside peripheral blood biomarkers would be particularly informative.

In conclusion, preoperative ESCA patients exhibited higher circulating $CD4^+CXCR5^+$ T-cell and $CD4^+CD25^+$ Treg phenotype frequencies than healthy controls, whereas early postoperative patients showed lower cellular phenotype frequencies than preoperative patients. Plasma CXCL13 levels were elevated in both patient groups relative to healthy controls. Elevated plasma CXCL13 was associated with deeper tumor invasion and shorter OS, and this association remained evident after adjustment for T stage in an exploratory Cox model. These findings support the potential value of plasma CXCL13 as a clinically feasible peripheral blood marker of adverse disease features in ESCA. Further studies integrating larger prospective cohorts, refined immunophenotyping, and tissue-level immune assessment are needed to clarify the biological basis and clinical utility of CXCL13-associated immune alterations in esophageal cancer.

Declarations

Ethical Approval and Accordance

The study protocol, including the retrospective use of residual clinical blood specimens and associated clinical data, was reviewed and approved by the Medical Ethics Committee of Affiliated Hospital of North Sichuan Medical College (approval no. 2026ER60-1). The study was conducted in accordance with the Declaration of Helsinki and applicable national and institutional guidelines and regulations. All specimens used in this study were residual EDTA-anticoagulated blood remaining after completion of routine clinical laboratory testing, and no additional blood was drawn solely for research purposes.

Consent to participate

The requirement for informed consent to participate was waived by the Medical Ethics Committee of Affiliated Hospital of North Sichuan Medical College because this retrospective study used residual clinical specimens remaining after routine laboratory testing and involved no additional blood collection solely for research purposes. No participants under 16 years of age were included in the study.

Consent to publish

Not applicable. The manuscript contains no identifiable personal information or images of individual participants.

Data availability

The de-identified individual-level clinical and laboratory data supporting the findings of this study are not publicly available because they contain potentially sensitive participant information and are subject to

institutional and ethical data-sharing restrictions. These data are available from the corresponding author upon reasonable request and subject to applicable institutional approval, ethical requirements, and data-protection regulations. Publicly available transcriptomic data used for the CXCR5 and CXCL13 analyses were accessed through the Gene Expression Profiling Interactive Analysis (GEPIA) web server (http://gepia.cancer-pku.cn; accessed December 17, 2025). The underlying public datasets comprised The Cancer Genome Atlas Esophageal Carcinoma dataset (project identifier: TCGA-ESCA), available from the Genomic Data Commons at https://portal.gdc.cancer.gov/projects/TCGA-ESCA, and matched normal esophageal tissue data from TCGA and the Genotype-Tissue Expression project (GTEx; dbGaP study accession: phs000424), available at https://www.ncbi.nlm.nih.gov/projects/gap/cgi-bin/study.cgi?study_id=phs000424.

Competing interests

All authors declare that they have no conflicts of interest.

Author contributions

S. L. designed the study. S. L., Y. L., B. G. and Q. L. contributed to data collection and laboratory measurements. S. L., G.L. and Y. L. analyzed the data. S.L. wrote the first draft of the paper. S. L. and M. A. M. reviewed and edited the manuscript. All the authors reviewed and approved the final manuscript.

Funding

This work was supported by the Scientific Research Development Fund of Affiliated Hospital of North Sichuan Medical College (2025LC011).

Clinical trial number

Not applicable. This study was not a clinical trial.

References

1. Bray F, Laversanne M, Sung H, et al. Global cancer statistics 2022: GLOBOCAN estimates of incidence and mortality worldwide for 36 cancers in 185 countries. CA Cancer J Clin. 2024;74:229–63. 10.3322/caac.21834.
2. Zhang R, Nie Y, Chen X, et al. A multicenter prospective clinical trial reveals cell-free DNA methylation markers for early esophageal cancer. J Clin Invest. 2025;135:e186816. 10.1172/JCI186816.
3. Li R, Huang X, Yang W, et al. Tertiary lymphoid structures favor outcome in resected esophageal squamous cell carcinoma. J Pathol Clin Res. 2022;8:422–35. 10.1002/cjp2.281.
4. Nakamura S, Ohuchida K, Hayashi M, et al. Tertiary lymphoid structures correlate with enhancement of antitumor immunity in esophageal squamous cell carcinoma. Br J Cancer. 2023;129:1314–26. 10.1038/s41416-023-02396-7.

5. Shen C, Fu Q. Follicular helper T cells (Tfh): heterogeneity in spatial distribution and phenotypic characteristics. Front Immunol. 2025;16:1686687. 10.3389/fimmu.2025.1686687.
6. Cui C, Wang J, Fagerberg E, et al. Neoantigen-driven B cell and CD4 T follicular helper cell collaboration promotes anti-tumor CD8 T cell responses. Cell. 2021;184:6101–e611813. 10.1016/j.cell.2021.11.007.
7. Liu W, You W, Lan Z, et al. An immune cell map of human lung adenocarcinoma development reveals an anti-tumoral role of the Tfh-dependent tertiary lymphoid structure. Cell Rep Med. 2024;5:101448. 10.1016/j.xcrm.2024.101448.
8. Tietscher S, Wagner J, Anzeneder T, et al. A comprehensive single-cell map of T cell exhaustion-associated immune environments in human breast cancer. Nat Commun. 2023;14:98. 10.1038/s41467-022-35238-w.
9. Wing JB, Lim EL, Sakaguchi S. Control of foreign Ag-specific Ab responses by Treg and Tfr. Immunol Rev. 2020;296:104–19. 10.1111/imr.12888.
10. Tang Z, Li C, Kang B, et al. GEPIA: a web server for cancer and normal gene expression profiling and interactive analyses. Nucleic Acids Res. 2017;45:W98–102. 10.1093/nar/gkx247.
11. Zheng Y, Chen Z, Han Y, et al. Immune suppressive landscape in the human esophageal squamous cell carcinoma microenvironment. Nat Commun. 2020;11:6268. 10.1038/s41467-020-20019-0.
12. Zhao L, Jin S, Wang S, et al. Tertiary lymphoid structures in diseases: immune mechanisms and therapeutic advances. Signal Transduct Target Ther. 2024;9:225. 10.1038/s41392-024-01947-5.
13. Liu Y, Ye SY, He S, et al. Single-cell and spatial transcriptome analyses reveal tertiary lymphoid structures linked to tumour progression and immunotherapy response in nasopharyngeal carcinoma. Nat Commun. 2024;15:7713. 10.1038/s41467-024-52153-4.
14. Huang H, Zhao G, Wang T, et al. Survival benefit and spatial properties of tertiary lymphoid structures in esophageal squamous cell carcinoma with neoadjuvant therapies. Cancer Lett. 2024;601:217178. 10.1016/j.canlet.2024.217178.
15. Zhai K, Xie R, Ru K, et al. Tertiary lymphoid structures correlate with the therapeutic efficacy and prognosis of resectable esophageal squamous cell carcinoma undergoing neoadjuvant chemoradiotherapy plus immunotherapy. Front Immunol. 2025;16:1616247. 10.3389/fimmu.2025.1616247.
16. Yeh CH, Finney J, Okada T, et al. Primary germinal center-resident T follicular helper cells are a physiologically distinct subset of CXCR5hiPD-1hi T follicular helper cells. Immunity. 2022;55:272–e2897. 10.1016/j.immuni.2021.12.015.
17. Song W, Craft J. T follicular helper cell heterogeneity. Annu Rev Immunol. 2024;42:127–52. 10.1146/annurev-immunol-090222-102834.
18. Qi J, Liu C, Bai Z, et al. T follicular helper cells and T follicular regulatory cells in autoimmune diseases. Front Immunol. 2023;14:1178792. 10.3389/fimmu.2023.1178792.
19. Le Coz C, Oldridge DA, Herati RS, et al. Human T follicular helper clones seed the germinal center-resident regulatory pool. Sci Immunol. 2023;8:eade8162. 10.1126/sciimmunol.ade8162.

20. Lu Y, Craft J. T follicular regulatory cells: choreographers of productive germinal center responses. Front Immunol. 2021;12:679909. 10.3389/fimmu.2021.679909.
21. Fahlquist Hagert C, Degn SE. T follicular regulatory cells: guardians of the germinal centre? Scand J Immunol. 2020;92:e12942. 10.1111/sji.12942.
22. Fattori S, Le Roy A, Houacine J, et al. CD25high effector regulatory T cells hamper responses to PD-1 blockade in triple-negative breast cancer. Cancer Res. 2023;83:3026–44. 10.1158/0008-5472.CAN-23-0613.
23. Shouse AN, LaPorte KM, Malek TR. Interleukin-2 signaling in the regulation of T cell biology in autoimmunity and cancer. Immunity. 2024;57:414–28. 10.1016/j.immuni.2024.02.001.
24. Cosgrove J, Novkovic M, Albrecht S, et al. B cell zone reticular cell microenvironments shape CXCL13 gradient formation. Nat Commun. 2020;11:3677. 10.1038/s41467-020-17135-2.
25. O'Connor RA, Martinez BR, Koppensteiner L, et al. Cancer-associated fibroblasts drive CXCL13 production in activated T cells via TGF-beta. Front Immunol. 2023;14:1221532. 10.3389/fimmu.2023.1221532.

Figures

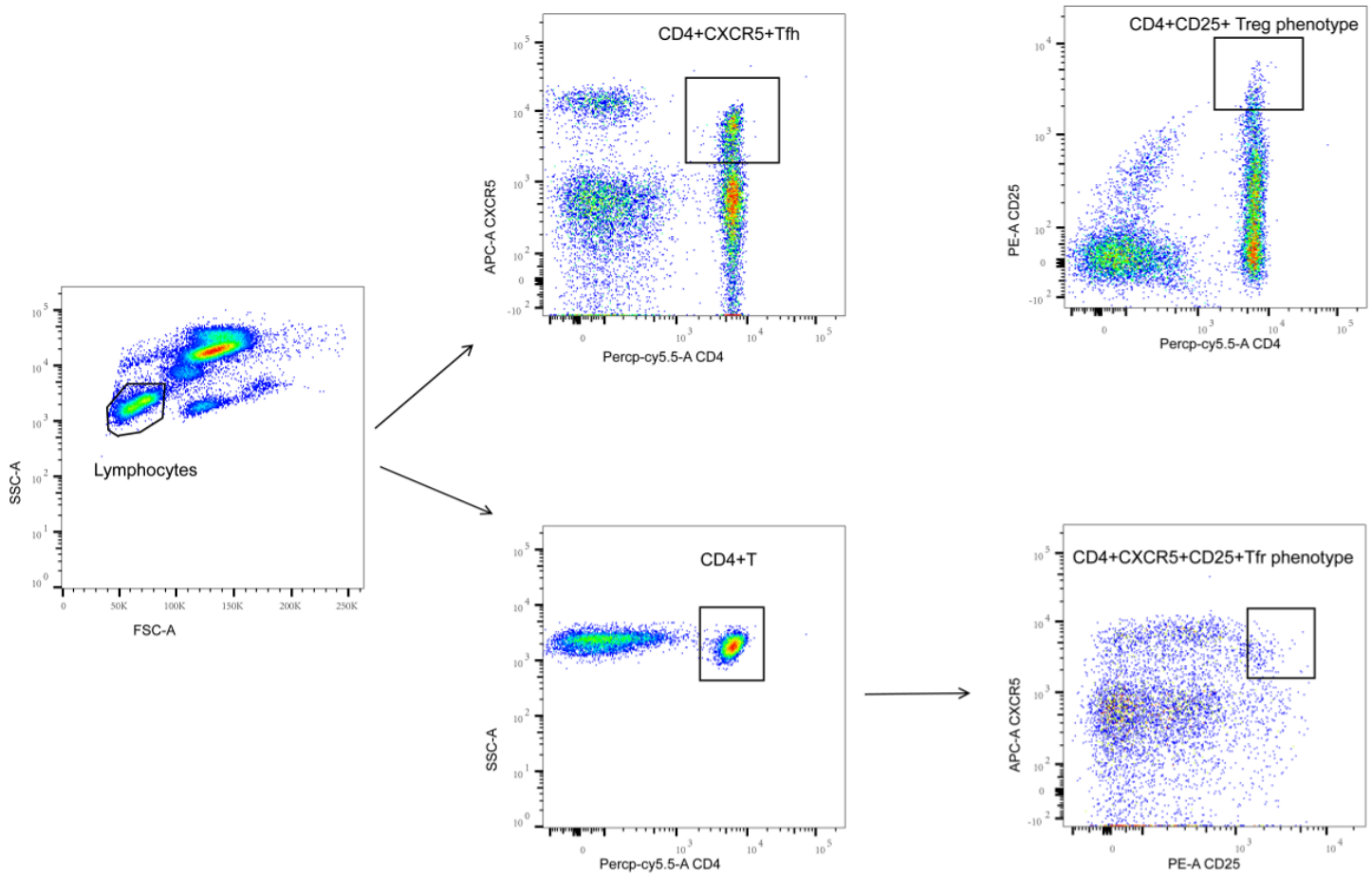


Figure 1

Representative flow cytometry gating strategy for circulating CD4⁺CXCR5⁺ T cells and CD25-based regulatory phenotypes

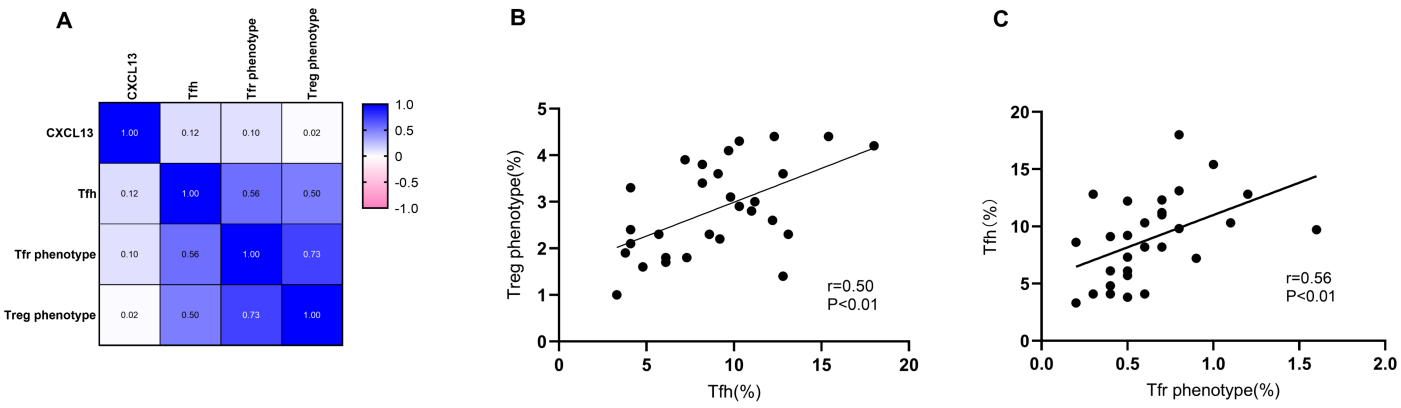


Figure 2

Correlation analysis of circulating CD4⁺CXCR5⁺ Tfh cells, CD25-based regulatory phenotypes, and plasma CXCL13 in preoperative ESCA patients

(A) Heatmap showing the Spearman correlation matrix among circulating CD4⁺CXCR5⁺ T cells, the CD4⁺CD25⁺ Treg phenotype, the CD4⁺CXCR5⁺CD25⁺ Tfr phenotype, and plasma CXCL13 levels in preoperative ESCA patients. The numbers within the cells represent Spearman's correlation coefficients (r). (B) Scatter plot showing a positive correlation between circulating CD4⁺CXCR5⁺ T-cell frequencies and the CD4⁺CD25⁺ Treg phenotype (r = 0.50, P < 0.01). (C) Scatter plot showing a positive correlation between circulating CD4⁺CXCR5⁺ T-cell frequencies and the CD4⁺CXCR5⁺CD25⁺ Tfr phenotype (r = 0.56, P < 0.01). Tfh, CD4⁺CXCR5⁺ T cells operationally defined as circulating Tfh cells; Treg phenotype, CD4⁺CD25⁺ cells; Tfr phenotype, CD4⁺CXCR5⁺CD25⁺ cells; CXCL13, C-X-C motif chemokine ligand 13; ESCA, esophageal cancer. P < 0.05 was considered statistically significant.

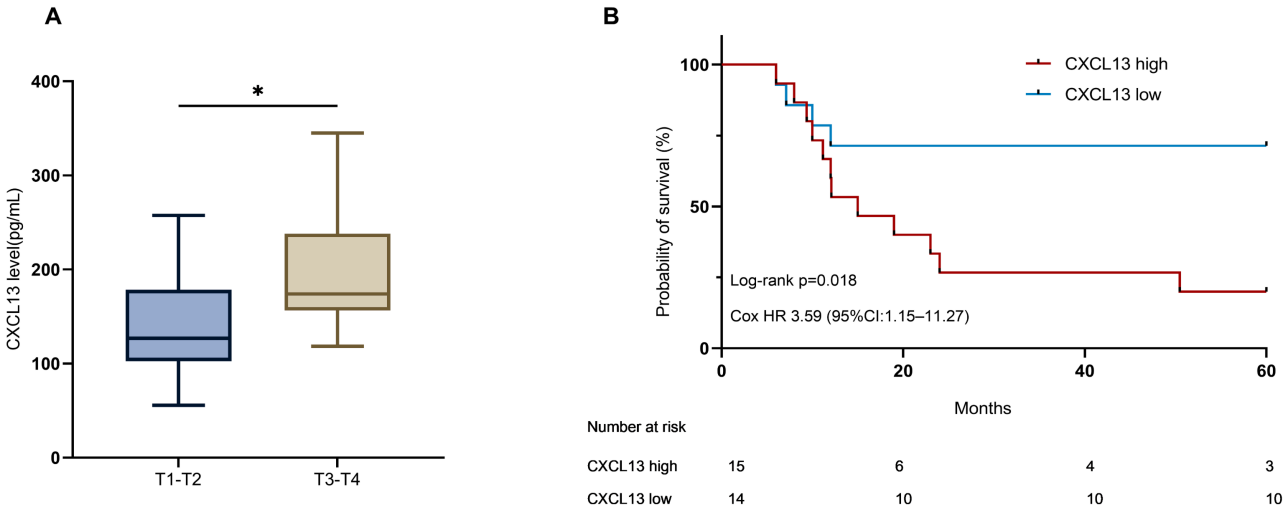


Figure 3

Association of plasma CXCL13 levels with tumor invasion depth and overall survival in patients with ESCA

(A) Plasma CXCL13 levels were compared between patients with early tumor invasion stage (T1–T2, n = 13) and advanced tumor invasion stage (T3–T4, n = 13). (B) Kaplan–Meier analysis of overall survival (OS) in preoperative ESCA patients with available follow-up data (n = 29), stratified according to the median plasma CXCL13 concentration. Patients were categorized into the CXCL13-high group (≥161.44 pg/mL, n = 15) and CXCL13-low group (<161.44 pg/mL, n = 14). Overall survival was administratively censored at 60 months. Survival curves were compared using the log-rank test. The hazard ratio (HR) and 95% confidence interval (CI) were estimated using univariable Cox proportional hazards regression. CXCL13, C-X-C motif chemokine ligand 13; ESCA, esophageal cancer.

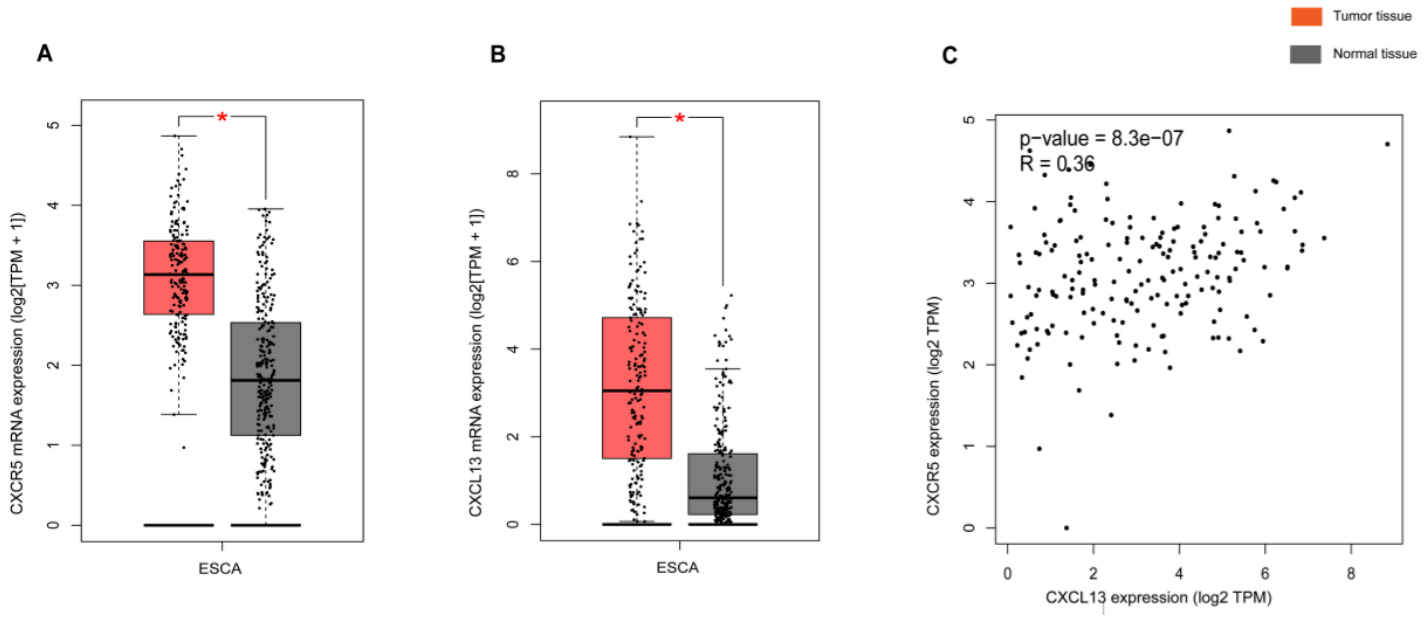


Figure 4

TCGA/GTEx-based transcriptomic analysis of CXCL13 and CXCR5 expression in ESCA tissues

(A, B) Box plots showing CXCR5 (A) and CXCL13 (B) mRNA expression in TCGA-ESCA tumor tissues (n = 182) and normal esophageal tissues from TCGA and GTEx (n = 286), as analyzed using GEPIA. Expression values are presented as $\log_2(TPM + 1)$. $P < 0.05$. (C) Pearson correlation analysis between CXCL13 and CXCR5 expression in TCGA-ESCA tumor tissues. CXCL13 expression was positively correlated with CXCR5 expression (Pearson's R = 0.36, $P = 8.3 \times 10^{-7}$). CXCL13, C-X-C motif chemokine ligand 13; CXCR5, C-X-C chemokine receptor type 5; ESCA, esophageal cancer; TPM, transcripts per million.